International Core Journal of Engineering Volume 6 Issue 2, 2020
ISSN: 2414-1895 DOI: 10.6919/ICJE.202002_6(2).0010

Simulation of PMSM Based on SVPWM in 60° Coordinate System

Yadong Cao [1, a], Wenbo Yuan [2, b]

[1] Shanghai Maritime University, Shanghai 201306, China;

[2] Shanghai Maritime University, Shanghai 201306, China.

[a]1904400487@qq.com, [b]630432808@qq.com.

Abstract

The permanent magnetic synchronous motor (PMSM) is widely used in many application scenarios, using Three-level inverter to drive permanent synchronous motors are more and more extensive. Due to the existence of trigonometric functions, traditional SVPWM in interval judgment and basic vector action time calculation is very complicated. This article has deeply analyzed the SVPWM technology and used SVPWM in 60° coordinate system to control permanent magnet synchronous motor system, reduced the complexity of the control system, and reduced the system uptime. The system was established by MATLAB/Simulink, and the simulation calculation was carried out to verify the method.

Keywords

SVPWM; PMSM; 60° coordinate system.

1. Introduction

Permanent magnet synchronous motor is a kind of motor whose rotor is a permanent magnet, and has a strong ability to resist motor torque disturbance. The motor has a simple structure, good running stability, and small size, so it is widely used in electric vehicles and industry. In applications, vector control methods are often used for permanent magnet synchronous motor control. The traditional SVPWM algorithm uses a lot of trigonometric functions and complex sector judgment logic. This article uses SVPWM at 60° coordinates to avoid a large number of trigonometric functions when determining the sector and calculating the action time of the basic vector, and applied to PMSM control system. The model was established by MATLAB/Simulink and simulation tests were performed to verify the feasibility of the method.

2. Mathematical model of permanent magnet synchronous motor

The three-phase winding of the motor flows into a sinusoidal current, which generates a rotating magnetic field. The interaction between the rotor magnetic field and the stator magnetic field causes the motor to rotate. The d-q coordinate system is also called a rotating coordinate system. It is a coordinate system commonly used by motors. The rotor is parallel to the q axis, and the d axis is perpendicular to the q axis. The d-axis direction is also the magnetic flux direction. Ignoring the core magnetic saturation and loss, the mathematical model of a permanent magnet synchronous motor is as follows[1]:

ISSN: 2414-1895
DOI: 10.6919/ICJE.202002_6(2).0010

$$\begin{cases} u_d = R_f i_d - \omega_e L_q i_q + L_d \dfrac{di_d}{dt} \\ \mathrm{u}_q = R_f i_q + L_q \dfrac{di_q}{dt} + \omega_e \left(\psi_f + L_d i_d\right) \\ J\dfrac{\mathrm{d}\omega}{dt} = T_e - T_L - B_f \omega \\ T_e = \dfrac{3}{2} p_n \left[\psi_f i_q + \left(L_d - L_q\right) i_q i_d\right] \end{cases} \quad (1)$$

In the formula: i_d, i_q, u_d, u_q are the d-axis and q-axis current and voltage, respectively; R_f is the stator resistance; L_d, L_q are the d-axis and q-axis inductance respectively; ψ_f is the flux chain of the permanent magnet; ω_e and ω are the electrical angular velocity and mechanical angular velocity of the rotor respectively; T_e is the electromagnetic torque, T_L is the load torque; J is the moment of inertia; B_f is the damping coefficient; P_n is the number of pole pairs of the motor.

3. Vector control principle in 60° coordinate system

3.1 Topology of NPC three-level inverter

Figure 1 shows the structure of a three-level inverter [2]. Three levels consist of three identical half-bridge converters, with diodes used for level clamping. The DC side of each half-bridge NPC is connected in parallel, and the AC end is connected to the corresponding three-phase AC system. u_{dc} is the DC-side voltage. Each phase of the inverter can output three level states: $u_{dc}/2$, 0, $-u_{dc}/2$. The three levels are represented by P, O, and N, respectively. The inverter has three phases, and each phase will have three level states, so for the entire three-level inverter, there are 27 output states, including 19 different voltage vectors, contains 19 different voltage vectors. These vectors are called basic vectors and can be equivalently synthesized as a reference voltage vector. As shown in Figure 2 [3-4], the basic voltage vector is divided into long vector, medium vector, short vector and zero vector according to the magnitude of the magnitude.

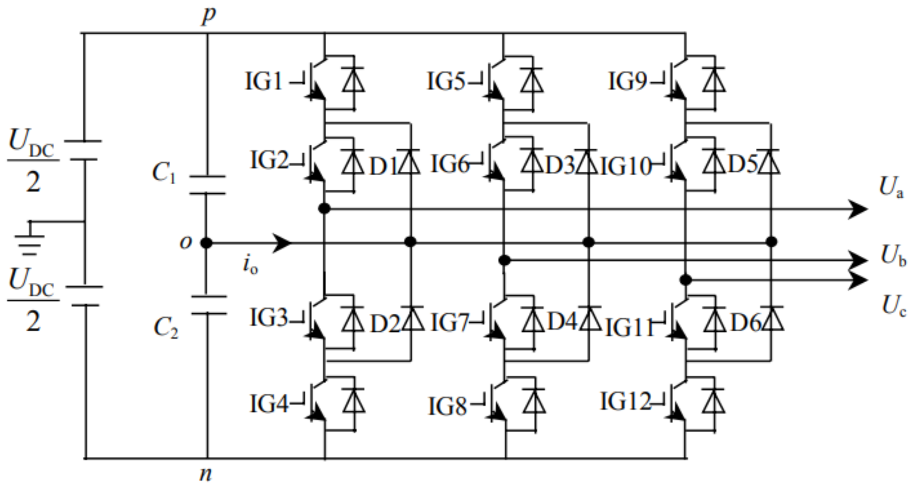

Figure 1. Structure of NPC three-level inverter

ISSN: 2414-1895 DOI: 10.6919/ICJE.202002_6(2).0010

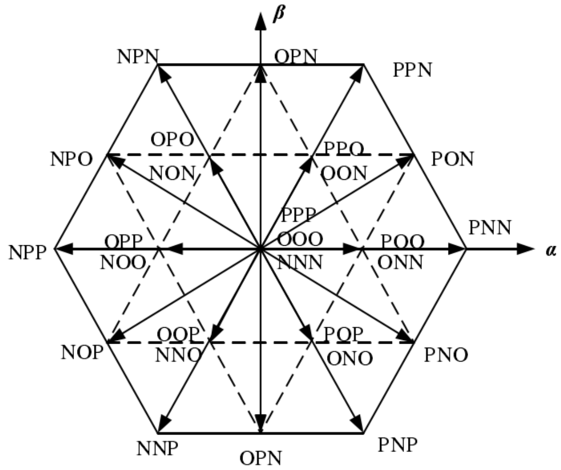

Figure 2. Three-level inverter space vector diagram

3.2 Coordinate Transformation and Standard Transformation

As shown in Figure 2, the entire space vector diagram is divided into six large sectors, and each large sector can be divided into six small sectors. Due to the symmetry of large sectors, a 60° non-orthogonal coordinate system can be directly used to perform interval judgment and calculate the basic vector action time. In the traditional algorithm modulation, the three-phase sinusoidal reference voltage is transformed into the α-β coordinate system through Park transform and Cark transform [5]. In the 60° coordinate system, it is defined that the g-axis coincides with the α-axis in the α-β coordinate system, and the h-axis can be obtained by rotating the α-axis in reverse of 60°, so that the g-axis is the horizontal axis and the h-axis is the vertical axis 60° coordinate system.

Model of α-β coordinate system transformed into *g-h* coordinate system:

$$\begin{bmatrix} V_g \\ V_h \end{bmatrix} = \begin{pmatrix} 1 & -\frac{1}{\sqrt{3}} \\ 0 & \frac{2}{\sqrt{3}} \end{pmatrix} \begin{bmatrix} V_\alpha \\ V_\beta \end{bmatrix} \tag{2}$$

In the formula, $\boldsymbol{V_a}$, $\boldsymbol{V_b}$, and $\boldsymbol{V_c}$ are three-phase voltages of the inverter, and $\boldsymbol{V_g}$ and $\boldsymbol{V_h}$ are coordinate values on the g-h coordinate system that undergoes coordinate changes. The magnitude of the small vector is $u_{dc}/3$,Normalize by using the magnitude of the small vector, and divide the coordinate value by $u_{dc}/3$ to obtain the normalized coordinate values $\boldsymbol{V_g^*}$, $\boldsymbol{V_h^*}$. Vector diagram of space in 60° coordinate system, as shown in Figure 3 [6-9].

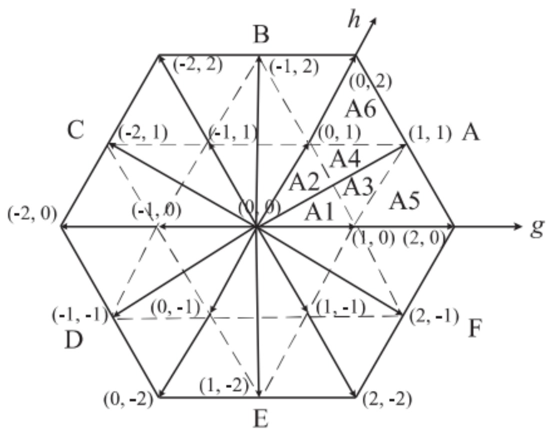

Figure 3. Vector diagram of space in 60° coordinate system

ISSN: 2414-1895
DOI: 10.6919/ICJE.202002_6(2).0010

3.3 Large sector judgment

As shown in Figure 3, the entire space vector diagram is divided into six large sectors, A to F. Similar to the orthogonal coordinate axis, the interval logical judgment in the 60° coordinate system is also processed by the coordinate value of the reference vector. In the non-orthogonal coordinate system, the coordinate values of the base vectors are all integers, and the calculation is quite simple. However, the 60° coordinate system is different from the 90° coordinate system. $\boldsymbol{V_g}^*<0$, $\boldsymbol{V_h}^*>0$ will occur in the large sectors of B and C. Therefore, an additional auxiliary line "$g+h=0$" is needed for judgment. Then when $\boldsymbol{V_g}^*+\boldsymbol{V_h}^*>0$, it is located in sector B; when $\boldsymbol{V_g}^*+\boldsymbol{V_h}^*<0$ <0, it is located in sector C.

The logic judgment rules for the interval where the reference vector is located are shown in Table 1. Among them, $\boldsymbol{V_g}^*$ and $\boldsymbol{V_h}^*$ are the abscissa and ordinate of a given vector after the standard transformation.

Table 1. Large range logical judgment table

N	$\boldsymbol{V_g}^*$	$\boldsymbol{V_h}^*$	$\boldsymbol{V_g}^*+\boldsymbol{V_h}^*$
A	>0	>0	
B	<0	>0	>0
C	<0	>0	<0
D	<0	<0	
E	>0	<0	<0
F	>0	<0	>0

3.4 Sector rotation

In the 60° coordinate system, the entire space vector voltage map is divided into six large sectors, each large sector is 60°. There are six small sectors in the large sector, and the division rules are consistent, so it has symmetry. When the reference vector falls in the Nth large sector, the sector can be rotated (N-1) by 60° to perform a uniform process. After consistent processing, the reference vectors of other large sectors can be rotated to sector A for simplified operations, and the coordinate model is rotated:

$$\begin{bmatrix} V_g^* \\ V_h^* \end{bmatrix} = \begin{bmatrix} 1 & 1 \\ -1 & 0 \end{bmatrix}^{N-1} \begin{bmatrix} V_g \\ V_h \end{bmatrix} \tag{3}$$

3.5 Small sector judgment

After the large sections are converted to the A sector, only the position of the reference vector in the A sector needs to be determined. A large sector is divided into six small sectors, as shown in Figure 4.

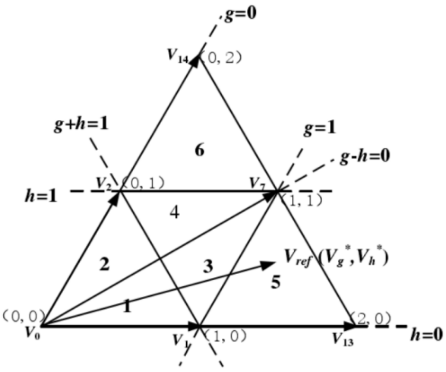

Figure 4. Schematic diagram of small sector division of sector A

ISSN: 2414-1895 DOI: 10.6919/ICJE.202002_6(2).0010

When judging the small sector to which the reference vector belongs, two auxiliary lines "g+h=1, g-h=0" need to be added to help the judgment. Referring to FIG. 4, the logical judgment of the small sector can be obtained as shown in Table 2.

Table 2. Small sector judgment table

n	V_g^*	V_h^*	$V_g^*+V_h^*$	$V_g^*-V_h^*$
1	<1	<1	<1	>0
2	<1	<1	<1	<0
3	<1	<1	>1	>0
4	<1	<1	>1	<0
5	>1	<1		
6	<1	>1		

3.6 Basic vector action time

After determining the small sector where the reference vector is located, the basic vector V_{ref} participating in the synthesis is determined. As shown in FIG. 4, the reference vector V_{ref} is represented by V_g^*, V_h^* coordinate values, and three nearby basic vectors can be equivalently synthesized. If the reference vector is in the small sector 5, it can be synthesized using the basic vectors V_1, V_7, and V_{13}. According to the principle of volt-second balance, the action time of these basic vectors can be calculated. Calculated according to the following relationship:

$$\begin{cases} T_1V_1+T_7V_7+T_{13}V_{13}=T_sV_{ref} \\ T_1+T_7+T_{13}=T_s \end{cases} \tag{4}$$

Solving the simultaneous equations above, the voltage vector action time is obtained;

$$\begin{cases} T_1=T_s(2-V_g^*-V_h^*) \\ T_7=T_sV_h^* \\ T_{13}=T_s(V_g^*-1) \end{cases} \tag{5}$$

In the same way, the basic vector action time of each cell can be calculated. The working time of the basic vector of each small sector is shown in Table 3.

Table 3. Basic vector action schedule of each small sector

n	T1	T2	T3
1,2	$T_sV_g^*$	$T_sV_h^*$	$T_s-T_s(V_g^*+V_h^*)$
3,4	$T_s-T_sV_h^*$	T_s-$T_sV_g^*$	$T_s(V_g^*+V_h^*)-T_s$
5	$2T_s-T_s(V_g^*+V_h^*)$	$T_sV_h^*$	$T_sV_g^*-T_s$
6	$2T_s-T_s(V_g^*+V_h^*)$	$T_sV_g^*$	$T_sV_h^*-T_s$

It can be known from the above logical operation table and model diagram that the sector judgment and calculation of the basic vector action time in the 60° coordinate system are very simple. The traditional SVPWM algorithm needs to use a large number of trigonometric functions, and the

ISSN: 2414-1895
DOI: 10.6919/ICJE.202002_6(2).0010

SVPWM algorithm in the 60° coordinate system can be implemented using only adders and multipliers, which improves the running speed and reduces the cost in the application.

After the above analysis, the simulation model of SVPWM in 60° coordinate system is shown in Figure 5.

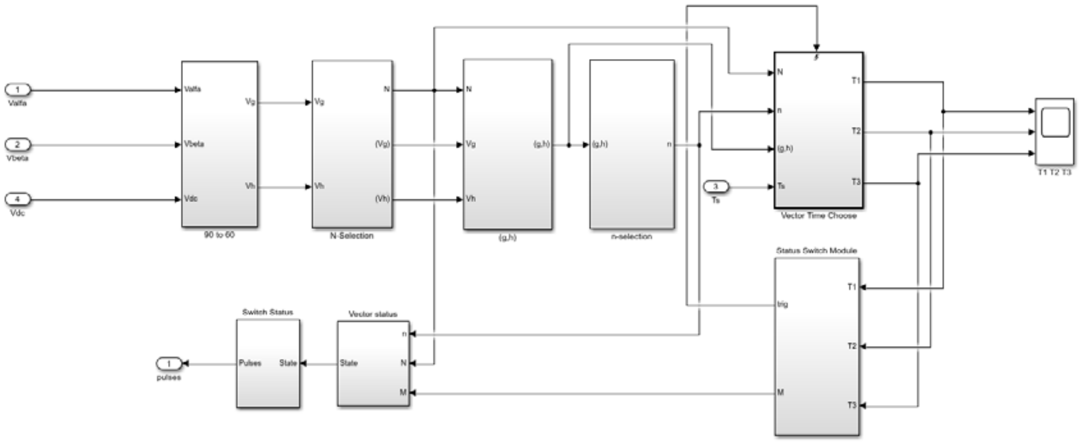

Figure 5. SVPWM simulation model of 60° coordinate system

4. Vector control of permanent magnet synchronous motor

4.1 Double closed loop control system

At present, there are many methods for vector control of motors. The control method with i_d=0 is the most commonly used and it is also the simplest and most effective [10]. Under this control method, the stator current acts on the *q*-axis, the larger *q*-axis current and the torque is more lager, and the response speed of the torque follows the current response speed.Therefore, when the electromagnetic torque is determined, the stator current passed is also determined, so unnecessary stator copper loss can be reduced, and the efficiency can be improved; In the control system, the symmetrical three-phase current is sinusoidal by detecting the rotor pole position as the control reference The waves form a smooth rotating magnetic field, and the stator current vector can be controlled on the *q* axis.

The schematic diagram of the permanent magnet synchronous motor vector control system is shown in Figure 6.

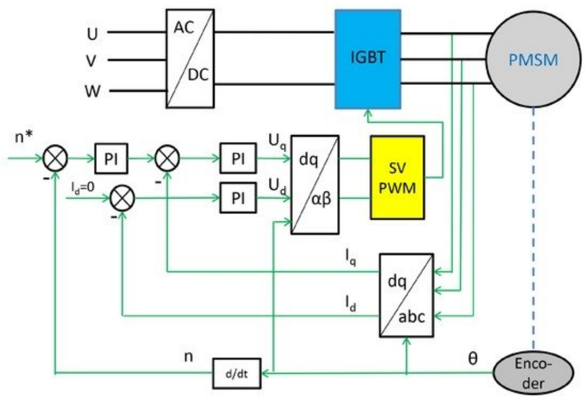

Figure 6. Schematic diagram of vector control system for PMSM

4.2 Controller PI setting

This system is a double closed-loop control system, which includes a speed loop and a current loop. The double closed-loop uses a traditional PI regulator. When designing the parameters of the speed loop, according to the expected bandwidth β of the speed loop, the active damping coefficient B_m can be introduced.

ISSN: 2414-1895 DOI: 10.6919/ICJE.202002_6(2).0010

$$B_m = \frac{\beta J - B_f}{1.5 P_n \psi_f} \tag{6}$$

The expression of the speed loop controller is

$$i_q^* = \left(K_{p\omega} + K_{i\omega}/s\right)\left(\omega^* - \omega\right) - B_m\omega \tag{7}$$

The parameters of the speed loop PI regulator can be set by the following formula:

$$\begin{cases} K_{p\omega} = \dfrac{\beta J}{1.5 p_n \psi_f} \\ K_{i\omega} = \beta K_{p\omega} \end{cases} \tag{8}$$

The current loop contains feed forward decoupling control, the expression is:

$$\begin{cases} V_d^* = (K_{pd} + K_{id}/s)(i_d^* - i_d) - \omega_e L_d i_q \\ V_q^* = (K_{pq} + K_{iq}/s)(i_q^* - i_q) - \omega_e (L_d i_d + \psi_f) \end{cases} \tag{9}$$

Among them i_q*, i_d*,V_d*, V_q*, ω* are reference signals. According to the method in [11], a parameter design strategy is provided, which greatly reduces the difficulty of parameter adjustment. The time parameter of the current loop is τ=min $\{L_d/R_f, L_q/R_f\}$, and the expected bandwidth of the current loop is $\alpha=2\pi/\tau$, The PI regulator parameter expression of the current loop is as follows.

$$\begin{cases} K_{pd} = \alpha L_d \\ K_{id} = \alpha R_f \\ K_{pq} = \alpha L_q \\ K_{iq} = \alpha R_f \end{cases} \tag{10}$$

5. System Simulation

In order to verify the correctness of the space vector control in the non-orthogonal coordinate system, a double closed-loop speed vector control system of speed was set up in MATLAB / Simulink for simulation experiments, as shown in Figure 7 [12-15]. The main parameters of the motor are shown in Table 4.

Table 4. Motor main parameters

The main parameters	Value
R_f	0.958Ω
Ψ_f	0.1827Wb
L_d	5.25mH
L_q	12mH
J	0.003Kg.m^2
B_f	0.008N·m·s
P_n	4

ISSN: 2414-1895 DOI: 10.6919/ICJE.202002_6(2).0010

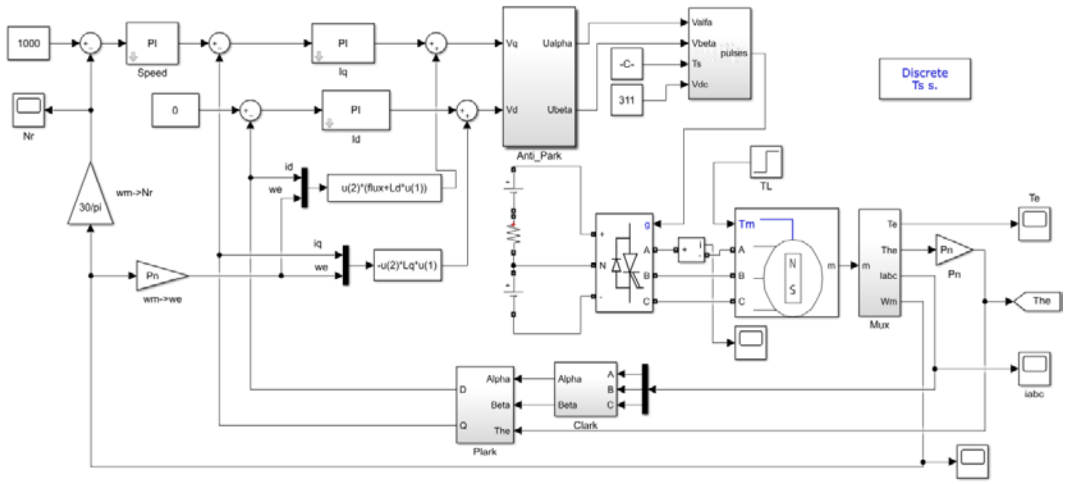

Figure 7. Simulation model of vector control system for PMSM

Inverter DC side voltage U_{dc} is 311V, and the sampling period of SVPWM is T_s = 0.0002s. According to the motor parameters, α=1100rad/s can be calculated. With the formula (10), the PI regulator parameters can be calculated, K_{pd}=5.775,K_{id}=K_{iq}=105.38, K_{pq}=13.2. Set the bandwidth of speed loop β=50rad/s, according to formula (6) and formula (8), we can calculate B_m = 0.013, $K_{p\omega}$ = 0.14, $K_{i\omega}$ = 7. The motor starts at no load. The set reference speed is 1000r/min. The load torque becomes 10N·m at 0.2 seconds, and the simulation time is 0.4 seconds.

The three-phase load current output by the voltage reference vector after 60° coordinate system vector space modulation is shown in Figure 8.

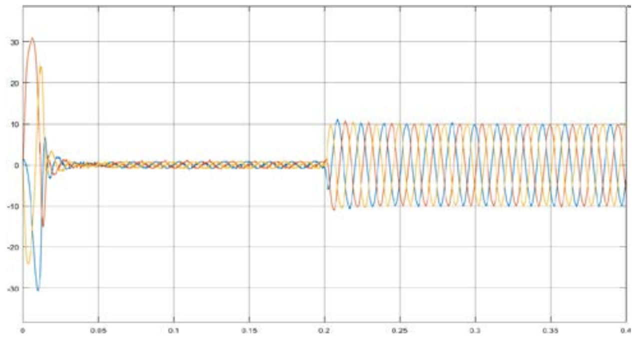

Figure 8. Three-phase load current

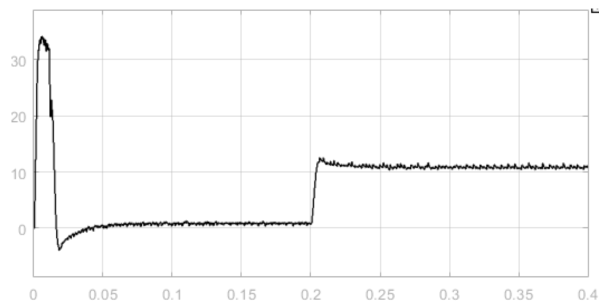

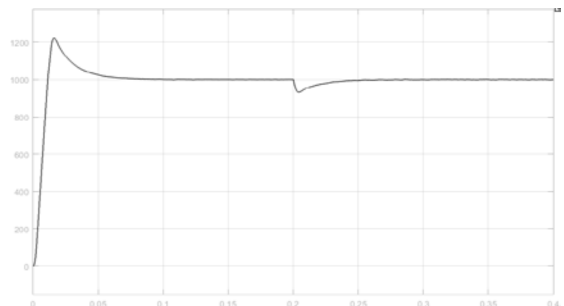

Figure 9. (a) Figure 9. (b)

Figure 9.(a) Torque waveform diagram in 60° coordinate system

Figure 9.(b) Waveform of rotation speed in 60° coordinate system

ISSN: 2414-1895
DOI: 10.6919/ICJE.202002_6(2).0010

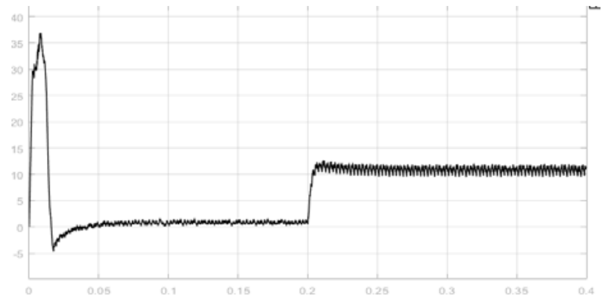

Figure 10. (a)

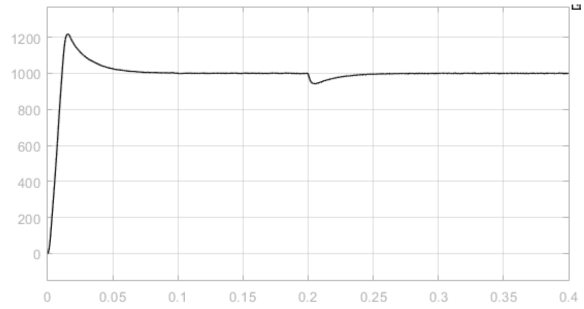

Figure 10. (b)

Figure 10.(a) Torque waveform diagram of traditional SVPWM algorithm

Figure 10.(b) Speed waveform of traditional SVPWM algorithm

Figures 9 are the torque waveform and speed waveforms of the motor, respectively. It can be seen from the simulation results that the torque and speed respond quickly, and after entering the steady state, the waveform is relatively stable. On this basis, the feasibility and good performance of the SVPWM control system in non-orthogonal coordinate system are verified. At the same time, when the external regulator parameters are unchanged, the control system using the traditional SVPWM algorithm is compared. Figure 10 are the torque waveform diagram and speed waveform diagram of the traditional algorithm, respectively.

According to the comparison, in the torque waveform diagram, the 60° coordinate system is more stable in steady state compared with the traditional algorithm. Some other parameters are listed in Table 5.

Table 5. Comparative Results

	Traditional SVPWM	60 ° coordinate
Torque adjustment time at startup	0.05s	0.04s
Speed adjustment time at startup	0.07s	0.07s
Speed overshoot during startup	21%	21%
Torque adjustment time at 0.2s	0.05s	0.05s
Torque overshoot at 0.2s	27%	25%
Speed adjustment time at 0.2s	0.03s	0.04s
Speed overshoot at 0.2s	5.9%	6.8%
Actual running time	14.64s	4.19s

According to the analysis of the above table, it can be known that in the 60° coordinate system, the performance indicators such as the adjustment time and overshoot amount of the system at no-load startup and torque conversion not only meet the standards of traditional algorithms, but also simplify the algorithm. With the same simulation parameter settings, the actual running time is reduced by two-thirds. In the application, the operating memory can be reduced and the running time can be reduced.

6. Conclusion

This paper analyzes the principle of a diode-clamped three-level inverter, discusses the vector control of a permanent magnet synchronous motor, and uses the space vector modulation method in a 60° coordinate system for the vector control system of a permanent magnet synchronous motor. The feasibility of SVPWM driving permanent magnet synchronous motor in 60° coordinate system was verified by Matlab / Simulink simulation. The control method of this scheme does not include complex trigonometric function calculations, has fast calculation speed and good dynamic

ISSN: 2414-1895 DOI: 10.6919/ICJE.202002_6(2).0010

performance, and provides a scheme for the application and development of permanent magnet synchronous motors.

References

[1] Ding Shuo, Cui Zongze, Wu Qinghui, et al. Simulation study of vector control of permanent magnetic synchronous motor based on SVPWM[J]. Foreign Electronic Measurement Technology, 2014, 33(6):81-85.(In Chinese).

[2] Zhao Gang, Wang Lei. Research of SVPWM Algorithm Based on Three-level Inverter [J]. Electric Drive, 2012, 42(11):26-29.(In Chinese).

[3] Wu Zhihong, Tao Shenggui, Cui Junguo, et al. Analysis on Topology Structure of Diode-clamping Multi-level Inverter [J]. Journal of Tongji University, 2003, 31(10):1217-1222.(In Chinese).

[4] Peng Haitao, He Zhiwei, Yu Haikuo, et al. Development Analysis on Permanent Magnet Synchronous Motor in Electric Vehicle[J]. Micromotors, 2010, 43(6):78-81.(In Chinese).

[5] Gou Bin, Feng Xiaoyun. Realization of SVPWM Method Based on 60° Coordinate System for Three-level Inverter [J]. Power Electronics, 2011, 45(5):65-66.(In Chinese).

[6] Zhao Hui,Li Rui, Wang Hongjun, et al. Study on SVPWM Method Based on 60° Coordinate System for Three-level Inverte[J]r. Proceedings of the CSEE, 2008(24):39-45.(In Chinese).

[7] Chen Xiaoou, Xu Chunyu, Wang Fengming. Study on SVPWM method based on 60° coordinate system for three-level inverter [J]. Advanced Technology of Electrical Engineering and Energy, 2017(02):46-52.(In Chinese).

[8] SUN Qiang, ZHAO Chaohui, ZHAN Jun, et al. Study on SVPWM Method Based on 60° Coordinate System for Two-Level and NPC Three-Level Inverter[J]. Electric Machines & Control Application, 2017(6).(In Chinese).

[9] X. Tang, X. Y. Yang, S. W. Zhao, et al. "Simulation of SVPWM overmodulation algorithm in 60° coordinate system," 2013 IEEE International Conference on Applied Superconductivity and Electromagnetic Devices, Beijing, 2013, pp. 367-370.

[10] Guan Liangyong, Xu Guoqing, Yuan Dengke. Design and Simulation of Vector Control System of Permanent Magnent Synchronous Motor[J]. Mechatronics, 2008, 14(12):51-53.(In Chinese).

[11] Harnefors L, Pietilainen K, Gertmar L. Torque-maximizing field-weakening control: design, analysis, and parameter selection [J].IEEE Transactions on Industrial Electronics, 2001, 48(1):161-168.

[12] S. Singh and A. N. Tiwari, "Analysis and simulation of vector controlled PMSM drive using SVPWM inverter," 2017 2nd International Conference for Convergence in Technology (I2CT), Mumbai, 2017, pp. 709-714.

[13] Li Yaohua, Liu Weiguo. Comparison of the VC and DTC for the PMSM [J]. Electric Drive, 2010, 40(10):9-12.(In Chinese).

[14] Ding Wen,Gao Lin, Liang Deliang, et al. Modeling and Simulation of Vector Control System for Permanent Magnet Syschronous Motors[J]. Micromotors, 2010, 43(12):66-71.(In Chinese).

[15] Wang Yang, Liu Yongguang. Simulation of PMSM with Vector Control Based on Simulation [J]. Modular Machine Tool & Automatic Manufacturing Technique, 2011(2):78-82.(In Chinese).